135

TYPE III SOLAR NOISE OBSERVED BELOW 100 kHz ON OGO 3

I. *Description of Events*

N. DUNCKEL and R. A. HELLIWELL

Radioscience Laboratory, Stanford University, Stanford, Calif. 94305, U.S.A.

and

J. VESECKY*

Center for Radar Astronomy, Stanford University, Stanford, Calif., U.S.A.
and Stanford Research Inst., Menlo Park, Calif., U.S.A.

(Received 14 February, 1972)

Abstract. Type III solar noise bursts have been observed in the frequency range 25–100 kHz with the VLF detector on OGO 3. The bursts decrease in frequency from 100 kHz (the highest frequency of observation) to as low as 25 kHz in approximately 45 min. The intensity at 100 kHz increases for about 20 min then decays over a period of approximately 1 h. The variation of the intensity with time becomes less regular at lower frequencies. Observed maximum intensities near 80 kHz range from 3×10^{-18} to 2×10^{-16} W m^{-2} Hz^{-1}. Bursts are predominantly associated with west-limb flares. Their commencement at 100 kHz tends to follow type III bursts observed at 2–4 MHz by about 10 min. Observed drift rates and decay times correspond roughly to those extrapolated from higher frequency measurements. Type III and the so-called 'high-pass' noise bursts often occur simultaneously, presenting a problem in identification. The solar noise events can be distinguished by their relatively slow time variation, smooth spectrum, and low intensity.

1. Introduction

Observations of type III solar noise are reported which represent the first comprehensive observations of type III noise below 450 kHz. With frequencies of observation extending to as low as 25 kHz, the region of the solar corona accessible to study is extended from about 0.2 to 1.0 AU. Moreover, the exciting possibility arises that the comparison of these low-frequency emissions with observations of the interplanetary medium will serve to test various emission theories.

According to the 'plasma hypotheses' of type III burst generation (Wild *et al.*, 1959), the emissions are caused by electrons having energies of about 40 keV and occur at the fundamental and/or the second harmonic of the plasma frequency. Recently other theories have been proposed in which the emission frequency is significantly greater than the local plasma frequency (Slysh, 1967 b; Papagiannis, 1971); in which the emission frequency is at the electron gyrofrequency and/or its second harmonic (Kuckes and Sudan, 1971); and in which generation at lower frequencies occurs predominantly at twice the plasma frequency (Haddock and Alvarez, 1971). Another suggestion is that the bursts are caused by protons (Smith, 1970; Graedel and Lanzerotti, 1971).

* Present address: Astronomy Department, The University, Leicester LE1 7RH, England.

Solar Physics **25** (1972) 197–209.

Ground-based measurements of type III solar noise bursts (Wild *et al.*, 1959; Boischot, 1967) are limited by the ionosphere to frequencies above about 5 MHz. Receivers on low-altitude satellites have observed type III noise bursts below this frequency but are still limited to frequencies above several hundred kilohertz by the high electron density of the surrounding plasma (Hartz, 1969; Alexander *et al.*, 1969; Fainberg and Stone, 1970a, b). Receivers on high-altitude satellites can in principle observe type III noise bursts to much lower frequencies. However, experiments which have thus far been reported in the literature have either suffered from a lack of data or have not included the lower frequency range (Slysh, 1967a,b; Haddock and Graedel, 1970).

A contribution of this paper is the distinction between type III solar bursts and an auroral-type noise called 'high-pass' noise (Dunckel *et al.*, 1970). High-pass noise occurs often during type III events with an intensity sufficient to completely prevent their detection. High-pass noise and type III solar noise both have spectra that extend down to a lower-cutoff frequency near 40 kHz. High-pass noise is observed mainly in or near the nightside of the Earth at $L > 5$ and exhibits a very high correlation with a measure of magnetospheric substorm activity called the auroral electrojet (AE) index.* High-pass noise has been observed in the magnetosphere, magnetosheath, and outside the shock boundary. (It may also have been observed on the Moon. High-pass noise was observed by OGO 3 at the same time that 200 kHz emissions of unknown origin were observed in the vicinity of the Moon by Slysh (1967b).) No satisfactory explanation for the generation mechanism of high-pass noise has yet been given but the evidence indicates a terrestrial origin. The high rate of incidence of high-pass noise during type III solar bursts may result from the triggering of magnetospheric substorms by associated solar flares.

Our results show that any study of type III solar noise bursts at low frequencies requires their clear discrimination from high-pass noise bursts. Type III solar noise may be identified by its smooth spectrum, by its slow, regular variation in intensity (especially above 50 kHz), and by its commencement about 10 min after the commencement of the event at 2–4 MHz. High-pass noise may be identified by its irregular spectrum, by its large fluctuations in intensity within periods of less than a minute, and by its close association with a high and/or increasing AE index.

2. The Experiment

The VLF package on the OGO 3 satellite consists of a loop antenna of 2.9 m diam driving four receivers which cover the frequency range 0.02 to 100 kHz. The satellite commenced to rotate 6 weeks after launch, but the direction of maximum sensitivity of the loop remained essentially unchanged during its rotation period. The receiver

* The AE index represents the difference in gammas between the maximum and minimum H-component readings at any of a number of high-latitude magnetometers (Davis and Sugiura, 1966). Microfilmed AE indices are available from the World Data Center A: Geomagnetism, Environmental Data Service, ESSA, Rockville, Md., U.S.A.

which produced all the data presented here swept the range 8–100 kHz in 2.3, 18, or 147 s depending upon the telemetry rate. Each sweep consisted of 256 spectral points. This receiver had a noise bandwidth of 800 Hz and a sensitivity of about 10^{-18} W m^{-2} Hz^{-1} at 100 kHz decreasing to about 10^{-17} W m^{-2} Hz^{-1} at 30 kHz. A calibration system injected harmonics of 1 kHz into the antenna every 16th sweep. A more complete description of this experiment is given by Ficklin *et al.* (1967). For the modes of operation used to study solar noise, the experiment is similar to that on OGO 1 (Dunckel and Helliwell, 1969).

A. CALIBRATIONS

Amplitude calibrations are based on pre-launch measurements. However, comparison of the level of the internal calibration signal soon after launch to that obtained 7 months later indicates that any change in power gain was less than 3 dB.

The power spectral densities quoted here refer to a linearly-polarized plane wave traveling in a vacuum and oriented with the magnetic field vector parallel to the axis of the loop antenna. Power readings obtained for a circularly-polarized wave arriving from a random direction should be increased by about 5 dB. The effect of the ambient plasma will also reduce the apparent power level. However, the error due to the presence of the plasma will be less than 3 dB for wave frequencies greater than 1.16 times f_p, the local plasma frequency.

3. Data

The output from the sweeping receiver is computer-processed and displayed on a cathode-ray tube where it is photographed by a movie camera. Each frame on the film displays one sweep. Figure 1 shows two examples of the output which have been photographed from the display and relettered. The upper panel shows type III solar noise and the lower panel high-pass noise, both recorded on the same pass. Each spectrum was obtained in 18 s. Samples of the background spectrum are shown for comparison in both examples. (The background spectrum in the lower panel includes a very weak high-pass burst.) They were recorded some minutes prior to the emission event and represent harmonic interference from the spacecraft inverter at 2.46 kHz superimposed on the receiver noise level.

The vertical scale is approximately logarithmic, adjacent tic marks representing differences of 10 dB. (The non-linear spacing of some tic marks is due to deviations from a truly logarithmic response in the receiver electronics.) The indicated scale factor is valid only at 80 kHz. At other frequencies the indicated power must be increased by 6 dB per octave below 80 kHz due to the response of the loop antenna.

The location of the satellite when the data of Figure 1 were being recorded is given by $R = 12.7/6.3\ R_E$ for the upper/lower panels, R being the geocentric distance; LMT = 20/19 h, LMT being the local mean time at the satellite in hours; and mlat = = 20/20 degrees, mlat being the magnetic latitude of the satellite. (The electron gyrofrequency is below the range covered by this receiver in all the examples presented.)

The spectrum of the solar noise burst shown in the upper panel of Figure 1 extends smoothly from a maximum in intensity near 100 kHz down to about 57 kHz, where it reaches the background level. As observed in a sequence of frames from our movie, the burst appears first at 100 kHz and rises rapidly to a maximum in intensity while it extends fairly smoothly to lower frequencies. The maximum in intensity drifts to progressively lower frequencies, and the minimum emission frequency decreases to about 35 kHz. Differences in power spectral density between individual spectra recorded 18 s apart are small, of the order of a factor of 2 or less near 100 kHz. (Other details of this burst will be discussed in connection with Figure 3.)

By comparison with the type III spectrum, the high-pass noise spectrum in the lower

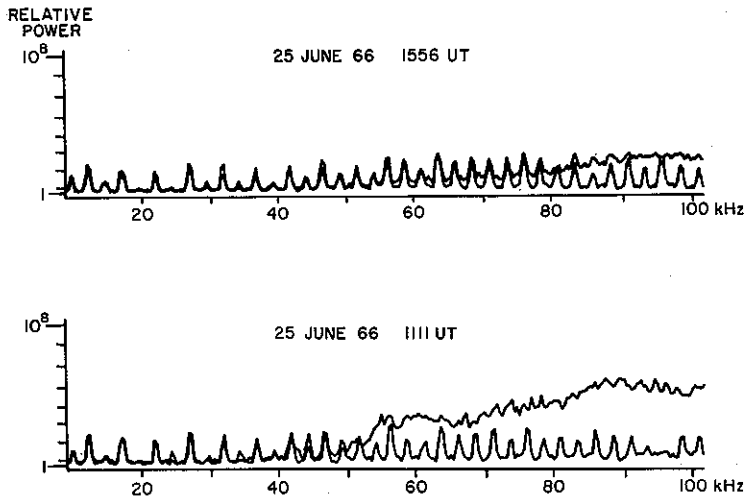

Fig. 1. Typical examples of type III solar noise (upper panel) and high-pass noise (lower panel) recorded on the same pass. Background noise spectrum including spacecraft interference is shown superimposed on both examples. High-pass noise spectrum appears similar to that of solar noise but is stronger and more irregular.

part of Figure 1 is stronger by a factor of about 200 at 95 kHz and is more irregular. Its low-frequency cutoff at 48 kHz is more abrupt. As observed in a sequence of frames from our movie, high-pass bursts tend to be observed first near 100 kHz and then to extend rapidly to lower frequencies, reaching 50 kHz in several minutes. The lower-cutoff frequency may vary erratically. Peaks in the spectrum may occur that are 10 dB above the average level; sometimes these appear to rise or fall in frequency at a rate of the order of 20 kHz/min. Differences in power spectral density between individual spectra recorded 18 s apart are of the order of a factor of 5 or more. No solar flares* were observed within an hour of the time at which this spectrum was

* Unless otherwise indicated, all solar flare data and solar noise data used in this study have been taken from *Solar-Geophysical Data*, published monthly by the Institute for Telecommunication Sciences and Aeronomy, ESSA, Boulder, Colo., U.S.A.

recorded. The AE index was high and increasing, rising from 403 γ at 1110 UT to 514 γ at 1120 UT. This association of high-pass noise with *increasing* AE index has been observed in several other cases.

Figure 2 shows the time behavior of a type III solar burst. The intensity-versus-time profiles were obtained by sampling each complete spectrum at the indicated frequencies. The sampling period is thus equal to the sweep time, which in this example is 147 s. Periodic peaks each 39 min are produced by the calibrate signal. This figure,

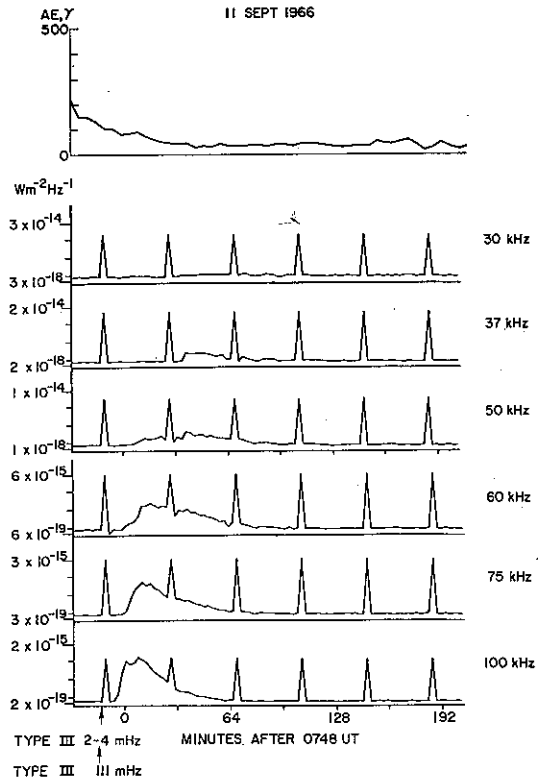

Fig. 2. Intensity-versus-time profiles of a type III solar burst. Periodic peaks are due to internal calibrate signal. Time profiles at frequencies above 50 kHz display rapid rise and slow decay typical of metric wavelength bursts but lower-frequency traces are irregular. Satellite location at 0734 UT: $R = 20\ R_E$; LMT = 17 h; mlat = 8°.

like the others that follow, was created from several photographs of the computer display; small optical distortions may be noted. Above the data is plotted the AE index in gammas at intervals of 2.5 min. This burst is one of the clearest and strongest yet observed. The event commences at 100 kHz at −6 min (with respect to 0748 UT) and descends smoothly to about 45 kHz. The lower cutoff remains at 45 kHz for about 20 min before extending to 30 kHz, which it reaches in about 5 min. Irregularities in the intensity appear more pronounced at lower frequencies. Ten minutes

prior to the first observation at 100 kHz a type III burst was observed at 111 MHz by the Potsdam Astrophysical Observatory (*Quarterly Bulletin on Solar Activity*). One minute after the 111 MHz observation the burst was observed at 2–4 MHz on the same satellite (Graedel, 1969). The burst is probably caused by a solar flare of importance 1– which was observed at 60° W solar longitude and which reached maximum within two minutes of the burst observations at 2–4 and 111 MHz.

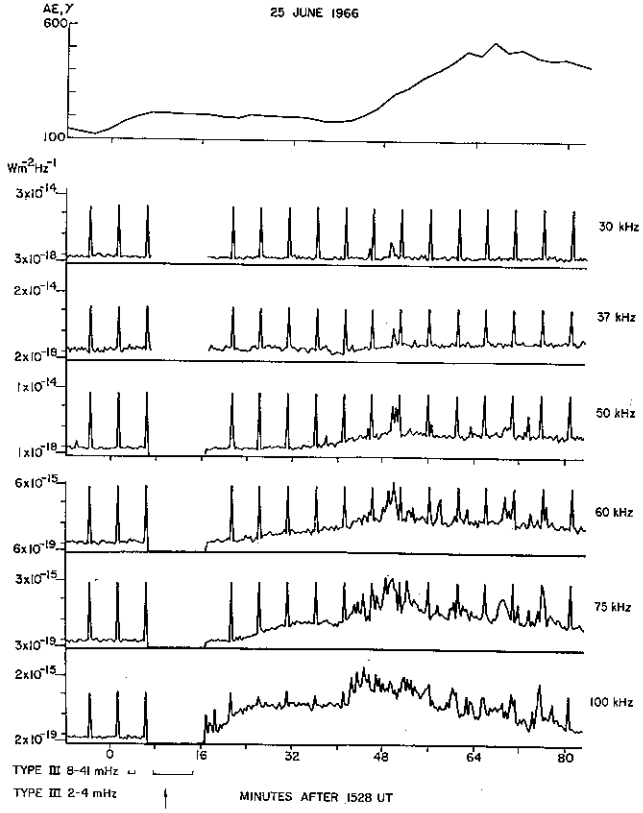

Fig. 3. Time behavior of type III event of Figure 1. Solar burst appears at 100 kHz following end of missing data at 16 min (after 1528 UT). At 43 min the 100 kHz level rises sharply and becomes irregular due to the superposition of high-pass noise associated with the commencement of the increase in AE index shown at top. Satellite location at 1600 UT: $R = 13\ R_E$; LMT = 20 h; mlat = 20°.

During this example no high-pass noise was observed. Its absence is probably related to the lack of commencing substorms as indicated by the auroral electrojet index, which is low and decreasing (from a maximum of 349 γ at 0645 UT).

Figure 3 shows the time profile of a type III burst which is contaminated by high-pass noise. It was recorded at a higher sweep rate (one sweep each 18 s) than the previous example and consequently the time scale appears expanded. Peaks due to the calibration signal recur each 4.9 min. The first 15 min of data represent back-

ground level. Data from 7 to 17 min (after 1528 UT) are missing. The type III solar noise burst is first observed at 100 kHz following the return of data at 17 min and reaches a peak about 10 min later. At lower frequencies the burst appears later and rises slower, reaching 37 kHz at about 42 min. No solar noise is evident at 30 kHz. At 43 min the 100 kHz level rises sharply and becomes much more irregular due to the added presence of high-pass noise. Simultaneously a substorm commences as indicated by the increasing AE index. The high-pass noise maintains a nearly constant lower-cutoff frequency of 50 kHz until 48 min, when its spectrum intensifies and extends briefly to 24 kHz to produce the peaks in the lower-frequency records. The intensity at 37 kHz due to type III noise is still increasing at the end of the record.

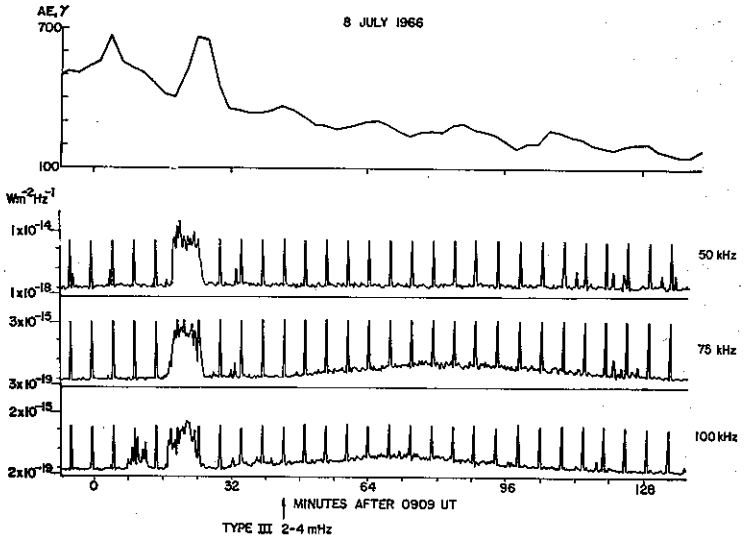

Fig. 4. Intensity-versus-time profiles showing both high-pass noise and type III noise. Strong high-pass burst causes sharp rise at all frequencies from 17 to 24 min (after 0909 UT). Type III burst causes slow rise commencing at 100 kHz at 29 min and at 75 kHz at 45 min. Note correlation of strong high-pass noise with high and increasing AE index. Satellite location at 10 UT: $R = 20\ R_E$; LMT = 21 h; mlat = 14°.

This low-frequency event follows the occurrence of type III solar noise bursts observed at 8–41 MHz by the University of Colorado radio telescope during the two periods indicated below the data. It also follows a type III burst (shown by the arrow) observed at 2–4 MHz by the radio-astronomy experiment on OGO 3 (Haddock and Graedel, 1970). All of these observations are probably related to the optical flare of importance 2B at 10° W solar longitude that reached peak intensity between 1538 and 1551 UT.

An unresolved type of disturbance appears at 100 kHz from 17 to 19 min. Since it displays a sharp cutoff at 92 kHz and its spectrum varies rapidly, it may be a weak high-pass noise burst. Similar events have been observed preceding other type III bursts.

Figure 4 shows the time profiles of a complex event in which both high-pass and type III noise were observed. Prior to 0909 UT + 7 min the data represent the background level (except for occasional weak bursts of unknown origin at 50 kHz). Following an enhancement from 8 to 14 min at 100 kHz probably due to high-pass noise, a strong high-pass noise burst occurs from 17 to 24 min at all frequencies shown. This burst coincides with a sharp rise in the AE index.

The type III burst reaches maximum intensity at 100 kHz at 72 min, 75 kHz at 88 min, and never reaches 50 kHz. It is unusual in that the intensity at 100 kHz has a double peak, the first occurring near 39 min and the second near 72 min. The time delay between onset and peak is much longer than usual, about 53 min as compared to the 10 min observed at 100 kHz in Figure 3. At 75 kHz the delay was also large. The lowest frequency excursion was about 55 kHz, the highest observed for any type III burst. A type III event at 2–4 MHz observed on the same satellite (Graedel, 1969) as well as an unidentified type of event at 23 and 111 MHz observed by the Potsdam Astrophysical Observatory (*Quarterly Bulletin on Solar Activity*) occurred at 0953 UT as shown by the arrow. The only solar flares observed during the period shown in Figure 4 occurred at 0336–1310 UT at 65° Wsolar longitude and at 0915–0935 UT at 11°W.

The fact that the high-frequency type III burst *follows* the onset of the low-frequency type III burst indicates that each results from a different source. A very slight inflection in the 100 kHz level 10 min after the HF burst indicates that the slow rise times may be the result of the superposition of two or more events. An alternative cause of the slow rise times is suggested by the unusually high lower-cutoff frequency. The solar wind density could have been so high that generation at 100 kHz occurred sufficiently far from the sun to cause the rise time to be similar to that usually observed at 50 kHz (compare Figure 2). Full understanding of this complex event, however, must await further study.

A. SUMMARY OF DATA

Thus far 13 definite examples of type III noise bursts have been discovered in an initial survey of the data. During these bursts the satellite was at $3 < R_E < 20$ and at $09 < \text{LMT} < 23$ h. Only one burst was observed when the satellite was in a position likely to have been in the solar wind; this burst resembled the others in appearance. High-pass noise was observed in the time period from ten minutes before to 1 h after the commencement at 100 kHz in 7 of the 13 cases. Six of the type III bursts were found by examining the data near the times at which type III bursts were observed at 2–4 MHz on the same satellite (Graedel, 1969). No low-frequency type III events were observed in conjunction with six other 2–4 MHz bursts. In three of the latter events, high-pass noise was present which could have prevented the observation of type III noise at low frequencies. In the other three events it is clear that no corresponding low-frequency type III bursts were observed.

The characteristics of the clearer of the 13 examples are as follows. The delay between the observation at 2–4 MHz and the onset at 100 kHz ranged from 9 to 14 min

(two examples in which the lf event preceded the hf event were excluded). The delay between the onset and the maximum at 100 kHz varied from 8 to 27 min with a median of 20 min. The median delay from the time of the hf burst to the time at which the lf event reached its minimum frequency was 62 min. The lower cutoff frequency varied between 25 and 55 kHz with a median of 40 kHz. The observed powers ranged from 3×10^{-18} to 2×10^{-16} W m^{-2} Hz^{-1}, with a median of 10^{-17} W m^{-2} Hz^{-1}.

Optical flares were observed 10 min before the 100 kHz onset time in all but two cases; the importance of these flares ranged from subflare to 3 with a median of 1.

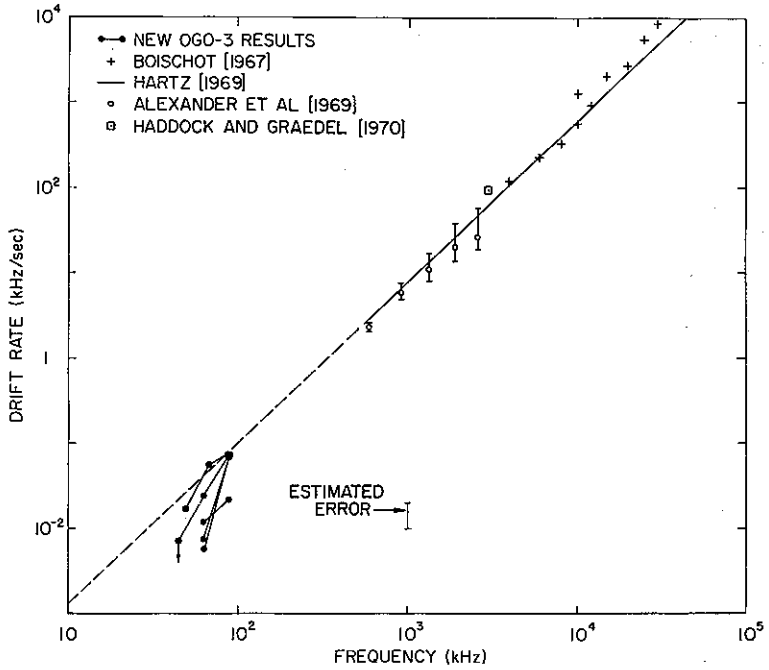

Fig. 5. Drift rates of type III bursts observed over a wide range of frequencies. Data from present study are shown by dots at lower left; lines connect data from single event. Low-frequency data fall close to simple extrapolation of high-frequency data. (Figure has been adapted from Alexander *et al.*, 1969.)

In the eight cases for which only one flare was active, the positions ranged from 10° to 70° West solar longitude with a median of 50°W. In contrast, the 2–4 MHz bursts which were not followed by low-frequency bursts were associated with flares whose positions, for the two cases in which they could unambiguously be ascertained, were 31° and 34° *East* longitude.

B. DRIFT RATES

The rate of change of frequency has been estimated for several of the clearer examples by measuring the time difference of maximum intensity at two frequencies spaced

closer than one octave. The results are shown in Figure 5. The approximate error in estimating the time of the intensity maxima is shown by the error bar. Drift rates at higher frequencies are plotted for comparison from data reported in the references. The line of best fit obtained by Hartz (1969) has been extrapolated (dashed line) to compare to the low-frequency data. A surprisingly good fit is obtained despite the considerable frequency range over which the relationship has been extrapolated. However, in the frequency range below 100 kHz, the drift rate appears to be smaller than that indicated at higher frequencies.

C. DECAY RATES

The *e*-folding time of decay has been estimated for several of the better examples of low-frequency type III bursts by estimating the slope of the burst decay from charts similar to those shown in Figures 2 through 4. Assuming that the power flux decays according to $e^{-t/\tau}$, as indicated by the theory of Jaeger and Westfold (1949), the decay constant τ is given by $0.43 \times$ (time required to decrease 10 db). The results, which appear in Figure 6 together with results from higher frequencies appear to fit the general trends of the higher-frequency data. The approximate error resulting from irregularities in the data is shown by the error bar; for the lowest frequencies the error may exceed this estimate.

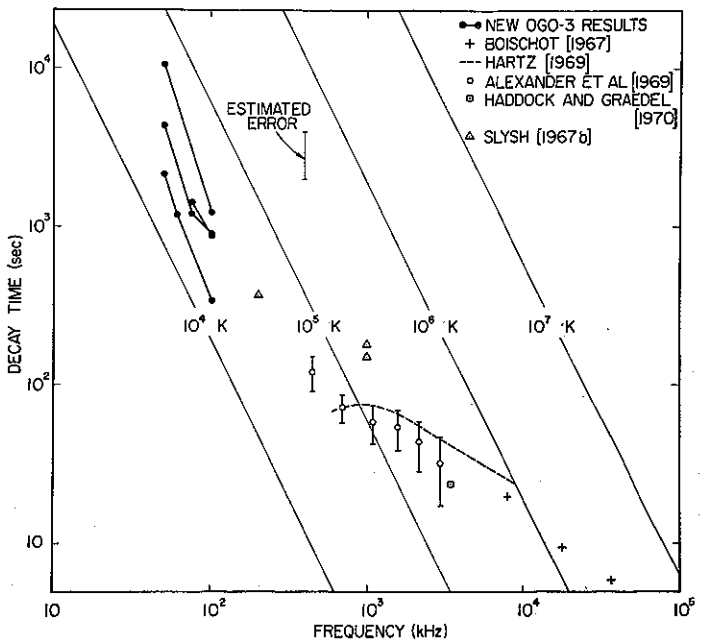

Fig. 6. *e*-folding decay times of type III bursts observed over a wide range of frequencies. Data from present study appear at upper left; lines connect data from single event. Lines of constant temperature were computed assuming decay was due to collisional damping of oscillations at the plasma frequency.

The isothermal lines drawn on this graph have been derived on the assumption that the decay results from the damping of oscillations at the plasma frequency by Coulomb collisions (Jaeger and Westfold, 1949). Under this assumption, electron temperatures of the order of 3×10^4 K are indicated at the lowest observed frequencies. This is a factor of 2 to 6 lower than satellite measurements at 1 AU (Kavanaugh *et al.*, 1970). Higher frequency measurements of type III noise bursts give temperatures that are similarly low with respect to other estimates (Hartz, 1969; Alexander *et al.*, 1969).

D. COMPARISON TO THE INTERPLANETARY MEDIUM

As mentioned in the introduction, the comparison of the present data to satellite measurements of the interplanetary medium may clarify the nature of the generation mechanism. For instance, plasma frequencies measured by Bame *et al.* (1970) near the times of several bursts were significantly lower than the observed lower-cutoff frequencies. It is not yet clear whether these observations indicate that generation is occurring at a frequency above the plasma frequency. It is quite possible that lower-frequency emissions occur but are shielded from the satellite by regions of high plasma frequency lying within the magnetosheath or magnetopause. The burst of Figure 3 occurs at the same time as energetic electron and proton events observed by Lin (1970). These and other relationships will be examined in a forthcoming paper. At present, the only generation mechanism that clearly does not fit the data is that based on generation at the electron gyro-frequency and its second harmonic (Kuckes and Sudan, 1971).

4. Conclusions

Type III noise bursts observed in the frequency range 25–100 kHz have the following characteristics:

(1) Above about 50 kHz their spectrum is smooth and slowly changing. The irregularity of the spectrum increases with decreasing frequency.

(2) Their drift and decay is comparable to that extrapolated from high-frequency bursts.

(3) They are closely associated with west limb flares, ground-based type III burst observations, and in some cases, with energetic interplanetary particle events.

(4) They tend to occur in association with type III bursts at 2–4 MHz which are related to flares in the western-hemisphere, but not with those which are related to eastern-hemisphere flares.

High-pass noise events appear during low-frequency type III noise bursts sufficiently commonly (during about $\frac{1}{2}$ of the observed events) that it is necessary to distinguish between the two types of events. High-pass noise events can be distinguished by the following characteristics:

(1) Their spectrum is rough and rapidly changing.

(2) Their lower-cutoff frequency fluctuates and may rise at the end of an event.

(3) They are closely associated with magnetospheric substorms, especially with substorm commencement as indicated by a high and/or rising AE index.

Acknowledgements

The work of the first two authors was supported by the National Aeronautics and Space Administration under contract NGR-05-020-288. That of the third author was supported by National Aeronautics and Space Administration contracts NGL-05-020-014 and NAS 5-11387.

Note added in proof: Simultaneous solar wind density measurements give further support to the suggestion that the characteristics of the burst of Figure 4 are due to unusually dense solar wind structure at large distances from the Sun. Explorer 33 data obtained from the MIT solar wind plasma experiment (through the National Space Science Data Center, Greenbelt, Md.) show that a region of dense solar wind plasma (f_p over 50 kHz) passed near the Earth at 05–06 UT on 8 July. Burst generation in this high density region could account for the elevated lower-cutoff frequency. Generation further from the Sun than usual would increase the risetime by allowing more time for spreading of the excitor packet.

Since many of the type III burst observations have taken place relatively close to Earth, it is possible that shielding by the Earth's plasma environment is responsible for the irregularities noted at the lowest frequencies. To what extent this occurs is not yet certain; however the gradual increase in irregularity with decreasing frequency show in Figure 2 suggests other causes.

References

Alexander, J. K., Malitson, H. H., and Stone, R. G.: 1969, *Solar Phys.* **8**, 388.

Bame, S. J., Felthauser, H. E., Hundhausen, A. J., Strong, I. B., Ashbridge, J. R., Gilbert, H. E., Smith, D. M., and Sydoriak, S. J.: 1970, *A Compilation of VELA 3 Solar Wind Observations, 1965 to 1967*, **1**, Los Alamos Scientific Laboratory Report LA-4536, October 1970.

Boischot, A.: 1967, *Ann. Astrophys.* **30**, 85.

Davis, T. N. and Sugiura, M.: 1966, *J. Geophys. Res.* **71**, 785.

Dunckel, N. and Helliwell, R. A.: 1969, *J. Geophys. Res.* **74**, 6371.

Dunckel, N., Ficklin, B., Rorden, L., and Helliwell, R. A.: 1970, *J. Geophys. Res.* **75**, 1854.

Fainberg, J. and Stone, R. G.: 1970a, *Solar Phys.* **15**, 222.

Fainberg, J. and Stone, R. G.: 1970b, *Solar Phys.* **15**, 433.

Ficklin, B. P., Stehle, R. H., Barnes, C., and Mills, M. E.: 1967, *The Instrumentation for the Stanford University/Stanford Research Institute VLF Experiment (B-17) on the OGO 3 Satellite*, Stanford Research Institute Report, May 1967.

Graedel, T. E.: 1969, *Dynamic Spectra of 4–2 MHz Solar Bursts: Results from Orbiting Geophysical Observatory III*, Final report, part 1, NASA contract NA5-2051, Dept. of Astromony Univ. of Michigan, Jan. 1969.

Graedel, T. E. and Lanzerotti, L. J.: 1971, *J. Geophys. Res.* **76**, 6932.

Haddock, F. T. and Graedel, T. E.: 1970, *Astrophys. J.* **160**, 293.

Haddock F. and Alvarez, H.: 1971, paper 4-1 presented in Commission V at the Spring Meeting of the U.S. National Committee of the International Union of Radioscience, Washington, D.C., April 8–10.

Hartz, T. R.: 1969, *Planetary Space Sci.* **17**, 267.

Jaeger, J. C. and Westfold, K. C.: 1949, *Australian J. Sci. Res.* **A2**, 322.
Kavanaugh, L. D., Jr., Schardt, A. W., and Roelof, E. C.: 1970, *Rev. Geophys. Space Phys.* **8**, 389.
Kuckes, A. F. and Sudan, R. N.: 1971, *Solar Phys.* **17**, 194.
Lin, R. P.: 1970, *Solar Phys.* **12**, 266.
Quarterly Bulletin on Solar Activity of the International Astronomical Union, published by the Eidgen. Sternwarte, Zurich, Switzerland.
Papagiannis, M. D.: 1971, *Solar Phys.* **18**, 311.
Slysh, V. I.: 1967a, *Astron. Zh.* **44**, 487 (*Soviet Astron. – A. J.* **11**, 389).
Slysh, V.I.: 1967b, *Kosmich Issled.* **5**, 897–910 (*Cosmic Res.* **5**, 759).
Smith, D. F.: 1970, *Solar Phys.* **15**, 202.
Wild, J. P., Sheridan, K. V., and Neyland, A. A.: 1959, *Australian J. Phys.* **12**, 369–398.